NASA Contractor Report 182185

An Experimental Study of Opposed Flow Diffusion Flame Extinction Over a Thin Fuel in Microgravity

Paul V. Ferkul

Case Western Reserve University
Cleveland, Ohio

February 1989

Prepared for
Lewis Research Center
Under Grant NGT-50088

National Aeronautics and
Space Administration

AN EXPERIMENTAL STUDY OF OPPOSED FLOW DIFFUSION FLAME EXTINCTION OVER A THIN FUEL IN MICROGRAVITY

Paul V.Ferkul*
Department of Mechanical and Aerospace Engineering
Case Western Reserve University
Cleveland, Ohio 44106

Summary

An experiment was conducted to examine the flame spread and flame extinction characteristics of a thin fuel burning in a low-speed forced convective environment in microgravity. The flame spread rate was observed to decrease both with decreasing ambient oxygen concentration as well as decreasing free stream velocity. A new mode of flame extinction was observed, caused by either of two means: keeping the free stream velocity constant and decreasing the oxygen concentration, or keeping the oxygen concentration constant and decreasing the free stream velocity. This extinction is called quenching extinction. By combining this data together with a previous microgravity quiescent flame study and normal-gravity blowoff extinction data, a flammability map was constructed with molar percentage oxygen and characteristic relative velocity as coordinates. The Damkohler number is not sufficient to predict flame spread and extinction in the near quench limit region.

Introduction

In the field of combustion, blowoff extinction has been widely studied. Blowoff occurs when the flow of reactants through the flame zone becomes so rapid that the chemical processes required for combustion are unable to keep pace. The reaction rate drops, and extinction soon follows. In terms of a nondimensional quantity, the ratio of characteristic flow time to chemical time becomes too small (the flow time is the amount of time spent by the oxidizer in the flame tip region and is inversely proportional to flow velocity). This ratio is called the Damkohler number.

The motivation for this work comes from that of T'ien (ref. 1) who presents a model of a stagnation point diffusion flame established over a solid fuel. The model includes radiative heat loss from the fuel surface. The governing equations are solved numerically, and the blowoff extinction phenomenon is observed as the velocity of the oxidizer becomes too large. However, of greater significance is the observation of another extinction limit, evident as the flow velocity becomes small. T'ien attributes this limit to flame temperature reduction as the rate of heat loss becomes significant compared with the rate of combustion heat release. Based on Arrhenius kinetics, the rate of chemical reaction is proportional to $\exp(-E/RT)$, where E is the activation energy, R the gas constant, and T the flame temperature. Thus, a significant reduction in flame temperature causes the chemical reaction rate to drop appreciably, thereby leading to extinction. The goal of this work was to observe this extinction (called quenching extinction) albeit in a different geometry.

Actually, the first work suggesting the importance of radiation in diffusion flame extinction was performed by Bonne (ref. 2). He concluded that radiative losses from the flame decreased the flame temperature substantially, thereby leading to extinction.

In order to observe quenching extinction, the flame requires a sufficiently slow flow of oxidizer into the flame zone. Unfortunately for this experiment, the normal gravitational environment of Earth induces natural convective flows leading to oxidizer velocities which are too large. For this reason, a microgravity environment was simulated by using the Zero Gravity Facility at the NASA Lewis Research Center. The entire experiment was dropped in vacuo down a 500-ft shaft and fell unrestricted for 5.18 sec. From the reference frame of the experiment, gravity no longer manifests itself and buoyancy forces are virtually eliminated.

An earlier experimental attempt to observe quenching extinction is described by Foutch (ref. 3), who used a hydrocarbon fuel (nonadecane) that is a solid at room temperature. The fuel was melted into a noncombustible fiber-frax sheet and allowed to solidify. The resulting fuel slab (1 mm thick) was ignited in a microgravity environment and moved into a prescribed oxidizer atmosphere to generate the flow velocity. Foutch was unable to observe extinction and concluded that the fuel was too thick to allow the flame to reach steady state in the 5.18 sec of microgravity time.

Recently Olson (ref. 4) conducted quiescent flame spread tests in microgravity on thin (0.0076-cm) paper samples (99 percent cellulose, 1 percent polyamide resin). The samples, measured at 3 by 15 cm, were ignited on a short side, and the flame was allowed to propagate. The flame propagation velocity V_F was measured. She found that a flame propagated in an oxygen-nitrogen environment of 21 mole % oxygen (which is almost identical to air), but a flame could not be established at 20.5 mole % oxygen. The low flow velocity recorded (0.54 cm/sec, simply V_F since from the flame's point of view the flow approaches at this velocity) is

*NASA Resident Research Associate.

substantially less than the velocity required to achieve blowoff in the same atmosphere of 21 mole % oxygen; this indicates that a quenching extinction was observed.

A recent theoretical analysis by Chen (ref. 5) examines the extinction characteristics of a flame established over the leading edge of a thin fuel plate in slow, forced convective flows in a microgravity environment. Chen observed quenching extinction as the oxidizer velocity became small, and he too attributed it to flame temperature reduction. As a result, the rate of radiant heat loss from the fuel surface outweighed the rate of combustion heat release.

Studying flames in microgravity provides basic scientific insight. With buoyancy greatly reduced, the effect of various flows (which in normal gravity may be masked by natural convection) can be more quantitatively studied. Furthermore, a comparison of flames in normal gravity and microgravity can be made, thus aiding the field of spacecraft fire safety.

Symbols

d distance normal to plate, mm

E activation energy

R universal gas constant

Re Reynolds number

T flame temperature

t time, sec

t_1 convective time scale, sec

t_2 viscous time scale, sec

u free stream velocity, cm/sec

V_{ch} characteristic relative velocity, cm/sec

V_F flame spread rate, cm/sec

x distance from leading edge, cm

ν kinematic viscosity

Experiment Description

Microgravity Environment

In order to achieve a microgravity environment, the Zero Gravity Facility at the NASA Lewis Research Center was utilized. This unique facility centers around a deep shaft dug into the Earth. The shaft houses a long cylindrical steel tube 6.1 m in diameter. When an experiment is dropped and allowed to fall freely down this tube, gravitational forces virtually disappear relative to its reference frame. However, in order to permit true free fall, aerodynamic drag must be eliminated. This is accomplished by evacuating the tube to 0.01 torr (1.3×10^{-5} atm). Any residual air drag will produce accelerations of less than 1×10^{-5} g. The microgravity time attained, which is limited by the depth of the tube, is 5.18 sec. A specially designed deceleration container filled with polystyrene beads stops the rapidly falling experiment gradually enough to prevent damage.

This experiment took place inside a combustion chamber (fig. 1) which can be filled with any desired oxidizer environment. The chamber is cylindrical in shape and has an internal volume of 113 liters. The experiment had to fit within the lower 25.4 cm of the vessel to allow its proper opening and closing. The camera port that was used is on the top; although farthest away from the experiment, it permits full visibility and allows truer perspective. The combustion chamber was mounted inside the drop package, the vehicle that contained the entire experiment.

Apparatus

The apparatus used in this experiment is shown in figure 2. It is the apparatus used by Foutch (ref. 3), with a few modifications.

Fuel.—As already mentioned, Foutch's fuel proved to be too thick. The flames were unable to reach steady state because much of the limited drop time went to bringing the fuel up to temperature.

To solve this problem, a much thinner fuel was needed. Thin cellulose sheets (laboratory wipes, 99 percent cellulose, 1 percent polyamide resin) having a half-thickness of 0.0038

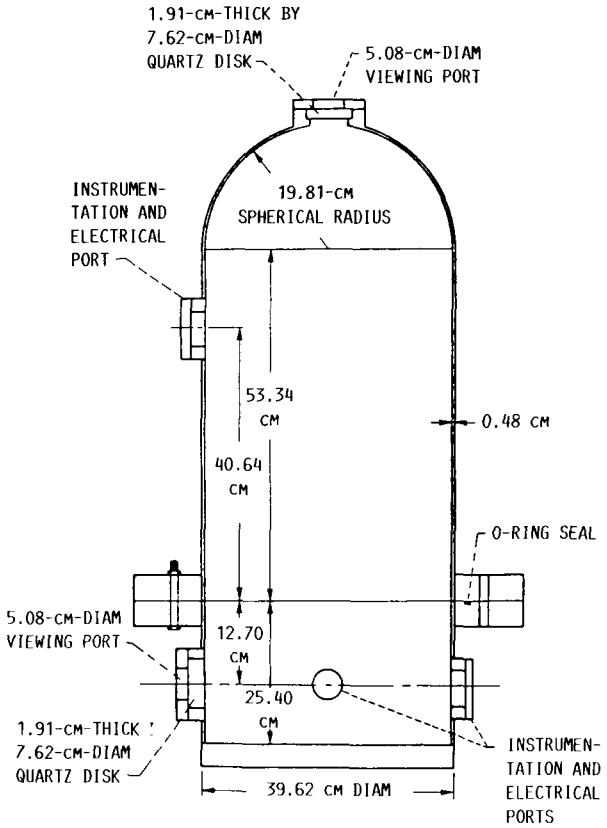

Figure 1.—Cross-sectional schematic of combustion chamber.

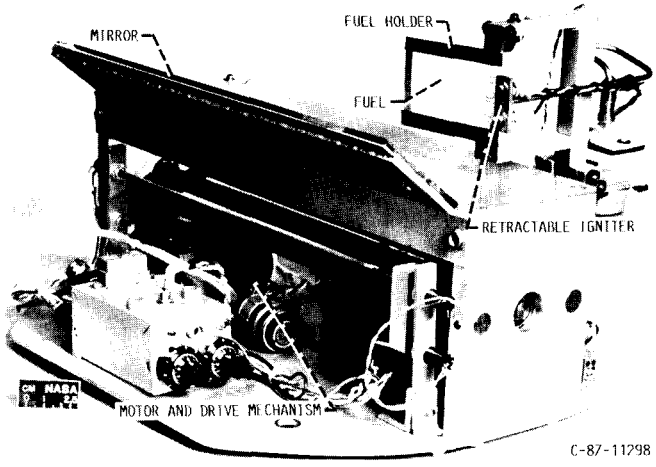

Figure 2.—Experimental apparatus.

cm and an area density, based on the half-thickness, of 1.00×10^{-3} g/cm^2 were chosen. This is the fuel first used by Olson (ref. 4); it was selected because she had good success with it and because a comparison with her work was desired. Furthermore, the same fuel width (3 cm) was used.

Generation of oxidizer velocity.—Instead of attempting to force the oxidizer past the paper fuel at a low speed, the fuel was moved at a constant speed through the oxidizer with a dc motor. The motor can produce speeds from 0 to 50 cm/sec, but 6.3 cm/sec covers the entire allowable distance in the 5.18 sec of microgravity time; thus a speed much higher than 6.3 cm/sec sacrifices valuable drop time. For example, if the sample were moved at 12 cm/sec, the fuel would reach the end of its allowable travel length at 2.7 sec into the drop. However, the ignition transient takes approximately 2 sec to fade, thereby leaving about 0.7 sec to obtain data. Although this may be sufficient time to obtain flame shape data, it is unlikely that the flame can reach extinction in such a short time. This time constraint was verified experimentally.

The leading edge of the sample was stiffened with a small piece of thin metal tape, which was creased and applied to both sides of the fuel so that the crease became the leading edge. This was done in order to prevent any flow disturbance downstream caused by the flimsy paper.

The sides of the paper were bounded by thin metal strips which held it in place (see fig. 3). A flame was established on the back of the sample to create the opposed flow mode of flame spread.

Flow field development.—The Reynolds number Re, based on the distance of the flame from the leading edge of the fuel sample and the sample velocity, varied from 30 to 450. Since the condition Re $>>$ 1 was not strictly met, a true Blasius boundary layer was not established. There is no simple analytical description of the flow field for this range of Reynolds numbers.

There were two additional complications. One was that the flow field was initially transient. The paper fuel was

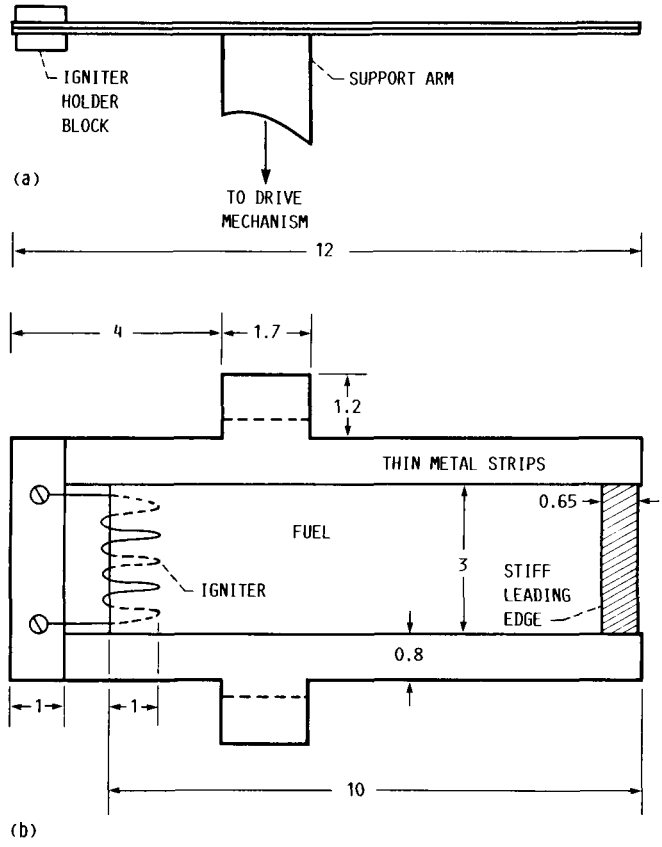

(a) Edge view.
(b) Front view.

Figure 3.—Schematic of fuel sample with fixed igniter. (All dimensions are in centimeters.)

accelerated rapidly from rest, so the flow field took time to develop. Ideally, the sample would be moved long enough to allow the flow field to develop; then the experiment would be dropped and the fuel ignited. However, because of the limitations imposed by the size of the combustion chamber, this approach was not possible.

The flow field development is commonly called impulsive motion of a semi-infinite flat plate. To estimate the time it takes for the flow to reach steady state, two important time scales are introduced (ref. 6). Let t be the time measured from the instant the plate is accelerated, u the plate velocity, x the distance of the flame from the leading edge, d an arbitrary distance normal to the plate, and ν the kinematic viscosity of the fluid; then t_1 and t_2 are defined as follows: $t_1 = x/u$ and $t_2 = d^2/\nu$. Here, t_1 is a measure of the time required for a point at a distance x downstream of the leading edge to sense the convective influence of the leading edge, and t_2 is a measure of the time required for the vorticity, generated at the surface of the plate when it is accelerated, to diffuse to a distance d from the plate. Clearly, if t/t_1 and t/t_2 are large, the flow has reached steady state. Because of the limitations of the chamber size and drop time, the largest value of t is 5.18 sec, which occurs at the end of the drop.

The value used for d was the flame standoff distance, because the leading edge region of the flame is most important in controlling flame spread and stabilization. As presented later, values of d ranged from 1.2 to 3.7 mm. The values of t_1 varied from 1 to 6 sec, and t_2, from 0.1 to 1 sec. Therefore, it is important to note that in some cases the time for the flow field to reach steady state was of the same order as the time of the experiment.

The second complication was that as the flame spread along the paper it was subjected to a changing velocity profile, even if the flow field had reached steady state. As distance from the leading edge decreased, the boundary layer thickness decreased. This was not a great problem since most of the flames spread quite slowly. To obtain an estimation of this effect, a Blasius boundary layer profile was assumed. In the worst case, the boundary layer thickness decreased 40 percent, though it usually changed by less than 10 percent.

The changing boundary layer thickness may have an effect on the flame if it is allowed to propagate far enough, but for the small flow velocities produced in this experiment, this effect needs to be better quantified. Of course, for large free stream velocities the flame may eventually be blown off as it spreads upstream into a thinner and thinner boundary layer with correspondingly higher and higher velocities occurring in the flame zone.

Figure 4 summarizes these effects. As explained in the section Results, the flames themselves do not appear to be greatly influenced by these complications.

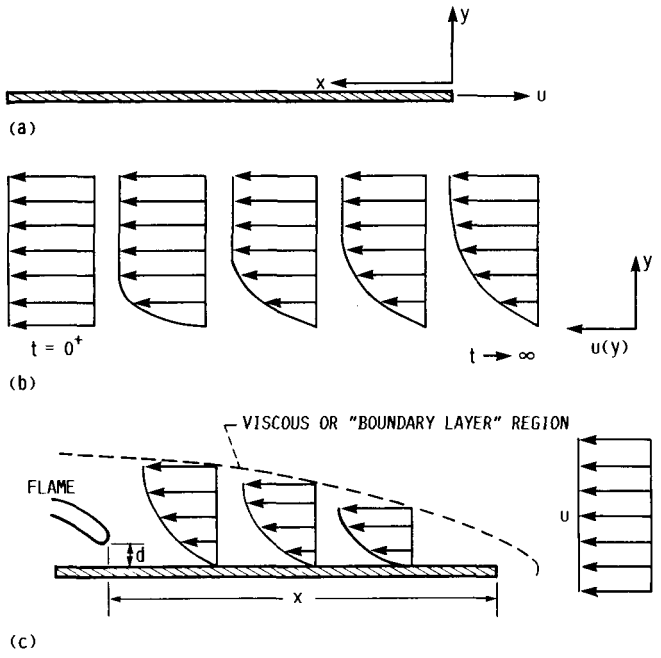

(a) Fuel plate attains an instantaneous velocity u at time $t = 0$.
(b) Velocity $u(y)$ at fixed x-location on plate as a function of time. Time increases from left to right.
(c) Velocity $u(y)$ as a function of distance along plate.

Figure 4.—Flow field.

Igniter.—The ignition characteristics were chosen to duplicate those in reference 4. A 0.0254-cm-diam Nichrome V wire was bent back and forth over the fuel as shown in figures 2 and 3. The igniter was positioned so that adjacent turns of the wire were on opposite sides of the paper. The wire typically had a resistance of 3 Ω and received power for 0.3 sec as a 28 V potential was applied. As determined in reference 4, this power input is enough to cause ignition yet minimizes the heat input to the system.

At first, the igniter was attached to the moving assembly (fuel and holder) to provide ignition after the sample was brought up to speed (fig. 3). However, the flames spread so slowly that they remained in the vicinity of the igniter, which acted as a heat sink, throughout the drop time. This problem was solved by using an igniter (fig. 5) which first moved with the fuel and ignited it and then slowly retracted out of the way. (No attempt was made to examine the effect of the retraction on the flow field.) To accommodate the new design, the fuel length was shortened from 10 to 7 cm. The shorter length sufficed since the flames spread so slowly.

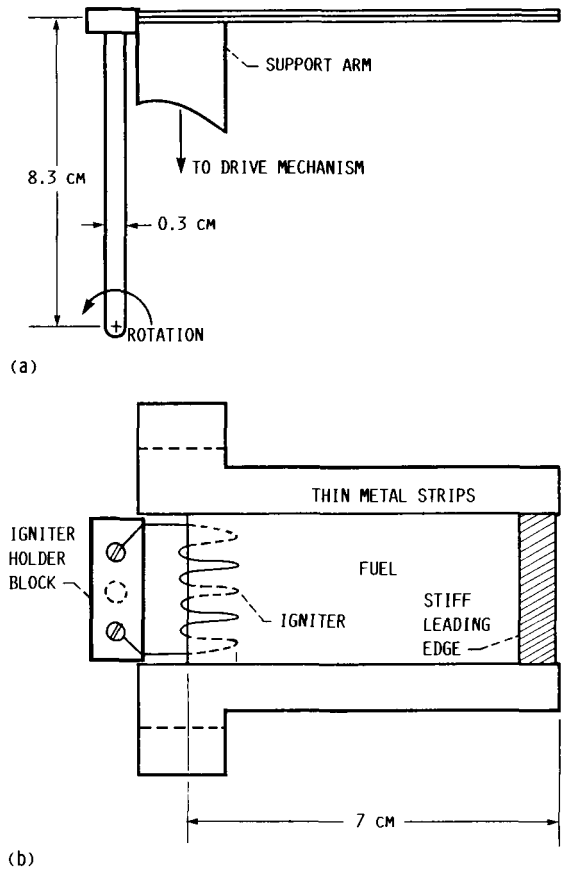

(a) Edge view.
(b) Front view.

Figure 5.—Schematic of fuel sample with moving igniter. (Other dimensions are as shown in fig. 3.)

Procedure

The fuel sample, with the stiffened leading edge, was mounted in the fuel holder. The apparatus was then placed in the combustion chamber, which was sealed and evacuated. The sample was left in a vacuum for at least 12 hr to remove moisture. After the chamber was filled with the desired (dry) oxidizer environment, the drop package was suspended at the top of the drop tube. Upon release the experiment began (time, $t = 0$). Within the test chamber the sample started to move at the chosen velocity, and the igniter received power. At $t = 0.3$ sec the ignition power was shut off. At $t = 1$ sec the igniter began to retract. Data were obtained from a Teledyne high-speed motion picture camera mounted on the top of the combustion chamber. In order to observe the dim blue flames, the most sensitive film which does not offgas (16-mm Kodak ektachrome high-speed video news S0251, 400ASA) was used. The f-number was 1.6, the shutter angle 160°, and the filming rate 24 frames/sec.

At $t = 5.18$ sec the drop package impacted the deceleration cart, and the experiment ended. The drop package was pulled up, and the film was retrieved. To further enhance the flame imaging, the film was force-processed at +2 f-stops.

Data were recorded with a film motion analyzer. A frame of the film was projected on a digitized screen with the frame number displayed. A cursor with a cross-hair sight, indicating the horizontal and vertical coordinates of the point in the cross hairs, was placed on the screen. At the press of a button, these data were fed directly into a computer data file for processing.

Results

Flame Spread Rates

The test parameters are presented in figure 6, which gives the measured flame spread rates as a function of oxygen mole fraction and characteristic relative velocity (including a point from ref. 4). All of these data are from microgravity tests, so the characteristic relative velocity includes only the vector sum of the fuel and flame spread velocities without any buoyant flow components. The symbols indicate the test condition for a given experiment. Four flame extinctions were observed within the 5.18 sec of microgravity time.

Next to each symbol appears the flame spread rate for that test condition. Spread rates of two flames were too small to be measured (<0.05 cm/sec). The spread rates of these two flames were undeterminable and are marked with a *U*.

In the absence of buoyant flows, spread rates increased uniformly with oxygen concentration and free stream velocity. In contrast, investigations of normal-gravity flames spreading over thermally thin fuels (ref. 7) indicate that for a given oxygen concentration the spread rates are either unchanged or decrease as free stream velocity increases, especially as the blowoff limit is approached.

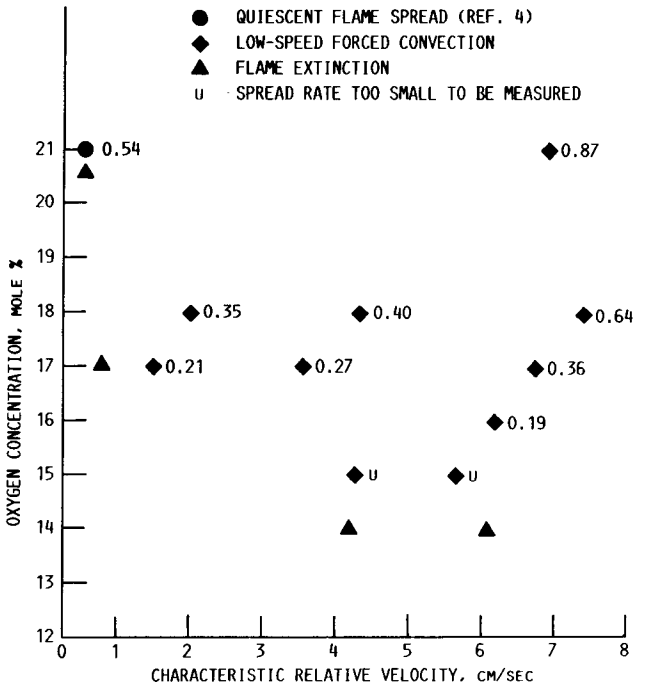

Figure 6.—Spread rates (in cm/sec) as a function of oxygen concentration and characteristic relative velocity in microgravity.

Flame Dimensions

The key flame dimensions extracted from the photographic record are shown in figure 7. A summary of the measurements from the experiments is shown in table I. The flame lengths and widths decrease both with decreasing oxygen concentration as well as free stream velocity (i.e., fuel speed). However, the standoff distance does not follow this simple trend. The flame standoff distance first increases as extinction is

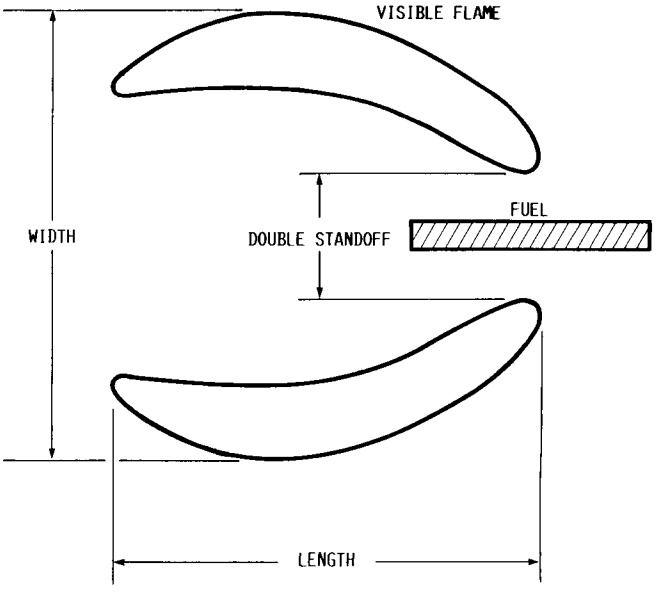

Figure 7.—Measured dimensions.

TABLE I.—FLAME DIMENSIONS

Oxygen content, mole %	Fuel speed, cm/sec	Spread rate, cm/sec	Double standoff distance,[a] mm	Length,[a] cm	Width,[a] cm	$\left(\frac{\text{Length}}{\text{Width}}\right)^{a}$	Extinction observed
21	6.06	0.87	2.4	3.5	2.2	1.6	No
18	6.75	.64	5.0	2.9	2.0	1.5	
18	3.92	.40	[b]7.5	[c]1.8	1.9	[c].9	
18	1.70	.35	[b]6.8	1.4	1.6	.9	
17	6.36	.36	6.0	2.5	1.9	1.3	
17	3.30	.27	[b]6.5	[c]1.7	1.7	[c]1.1	
17	1.31	.21	6.0	[c]1.5	[c]1.4	1.1	
17	.81	---	---	---	---	---	Yes
16	5.96	.19	5.9	2.2	1.7	1.3	No
15	5.66	(d)	5.0	1.5	1.3	1.1	No
15	4.29	(d)	[c]5.5	[c]1.1	[c]1.2	.9	No
14	6.08	---	---	---	---	---	Yes
14	4.19	---	---	---	---	---	Yes

[a]Approximately constant unless otherwise noted.
[b]Slightly increasing.
[c]Slightly decreasing.
[d]Unmeasurably small.

approached (decreasing velocity and/or oxygen percentage), but then decreases slightly close to the limit. As indicated in table I, some of the dimensions were slightly increasing or decreasing at the end of the 5.18 sec of test time, but in all cases the dimension recorded is the one that occurs just prior to the end of the experiment.

A representative sample of the data is given in figures 8 to 12. Fuel location, flame location relative to the fuel, double standoff distance, flame length, and flame width, all as a function of time, are shown for the data point having 17 mole % oxygen and a characteristic relative velocity of 1.52 cm/sec. The fuel location and flame location data yield the fuel velocity and flame spread rate, respectively.

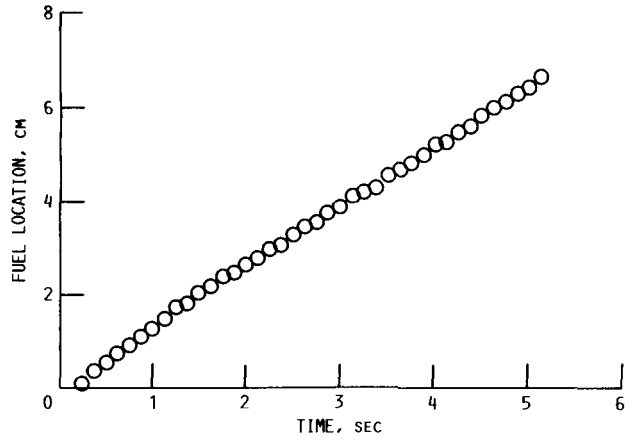

Figure 8.—Fuel location as a function of time for oxygen concentration = 17 mole % and V_{ch} = 1.52 cm/sec.

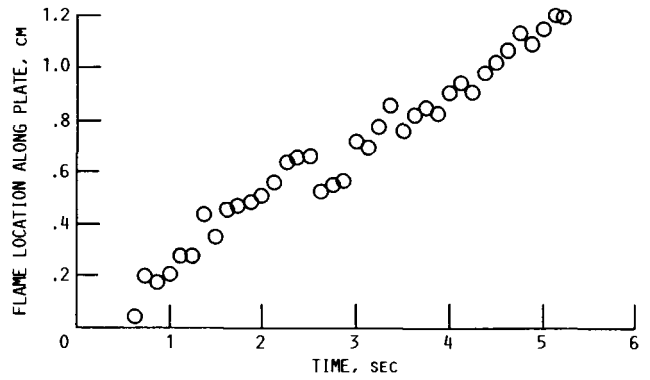

Figure 9.—Flame location as a function of time for oxygen concentration = 17 mole % and V_{ch} = 1.52 cm/sec.

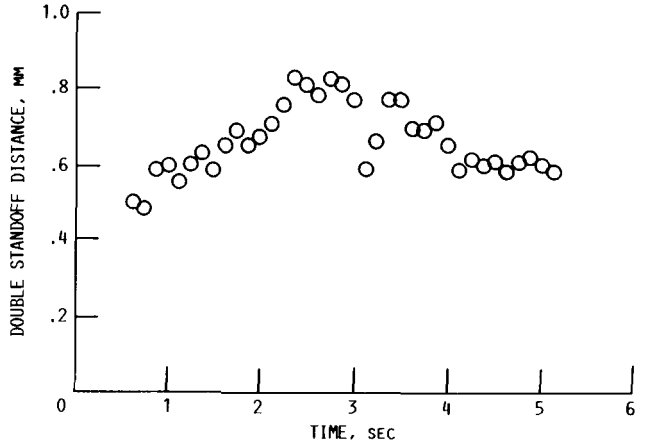

Figure 10.—Double standoff distance as a function of time for oxygen concentration = 17 mole % and V_{ch} = 1.52 cm/sec.

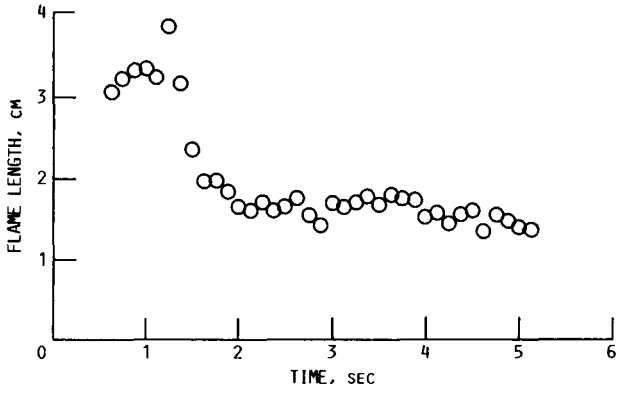

Figure 11.—Flame length as a function of time for oxygen concentration = 17 mole % and V_{ch} = 1.52 cm/sec.

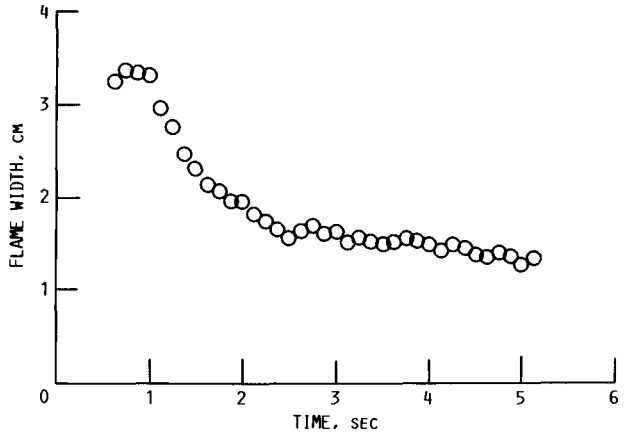

Figure 12.—Flame width as a function of time for oxygen concentration = 17 mole % and V_{ch} = 1.52 cm/sec.

The effect of ignition for this particular test condition can be seen in figures 9 to 12. During ignition, the flame was quite strong and yellow, thereby indicating that it was hot enough to induce soot formation. Figure 9 shows the flame spreads more quickly initially, as indicated by the steeper slope of the data points. In figure 10 the standoff distance initially increased as the strong, ignition-influenced flame began to weaken and move farther from the fuel surface. In figures 11 and 12, the flame length and width peak at some ignition-induced maximum value and then decrease and level out. These four figures suggest that ignition effects fade about 2 sec into the test. The error analysis appears in the appendix.

Flame Photographs

A visual comparison of flames spreading in microgravity is shown in figures 13 and 14. Two views of each flame are shown. The bottom photo shows an edge view of the fuel sample with the relative free stream velocity blowing from right to left. This view provides the maximum optical depth for viewing the two-dimensional flame. The top photo shows the flame as it appears looking down on the fuel sample (front view), which appears as a plane rectangle. This view is used mainly to check that the flame is two-dimensional, however some flames are so weak that they are not visible in this view.

As mentioned in the description of the apparatus, two different fuel lengths, 7 and 10 cm, were used. Only half a flame is presented in the bottom photos of the longer fuel samples because the support arm of the fuel sample holder obscured part of the other half (see fig. 3). Note also that for the longer fuel sample, the igniter was stationary relative to the sample and can still be seen glowing dim red downstream of the flame. This was the primary reason for modifying the apparatus to allow for a retractable igniter. Because the flames spread so slowly, the igniter remained close to the flames, acted as a heat sink, and could quench weak flames. The tests using the longer samples were not repeated once the retractable igniter was devised because the flames involved were far enough from the extinction limit to be relatively unaffected by the presence of the igniter wire.

Some general observations can be made from the collected flame photos. For a fixed oxygen percentage the flames become stronger (judged by flame brightness) as the free steam velocity is increased, and for a fixed free steam velocity the flames become stronger as the oxygen percentage is increased. Since the flame dimensions and appearance tend to stabilize, the development of the boundary layer on the sample does not seem to significantly influence the flames throughout the test.

The photos also show that all the flames except one (i.e., 21 mole % oxygen, 6.93 cm/sec in fig. 14) appear to be soot-free, judged by the absence of yellow in the flame color. Some of the flames are very dim blue, with the front view not visible at all. Although temperature measurements were not made, the flame colors can be a qualitative indicator. In general, the flames became dimmer as the oxygen percentage or free steam velocity was decreased. A dimmer flame suggests a lower flame temperature.

Flame Extinctions

Figure 15 presents the flames observed just before extinction for the three conditions when extinction occurred. Immediately following ignition, these flames reached their peak intensity and then waned throughout the test. After becoming quite small, portions of the flame went out, and the fuel sample in these regions began to smolder. This is evident as small red spots in both views of two of the flames. After the flame went out completely, the remaining smoldering began to diminish and disappear. The time it took for the flame to go out, measured from the start of the drop, was at least 4 sec.

One of the photos does not demonstrate this characteristic smoldering. In this case, the photo is one that was taken prior to the initiation of smoldering in order to capture the flame, since this particular flame became too dim to view prior to extinction. In other words, the flame shown weakened to the point of not being visible; then, about 1 sec later, visible

ORIGINAL PAGE
COLOR PHOTOGRAPH

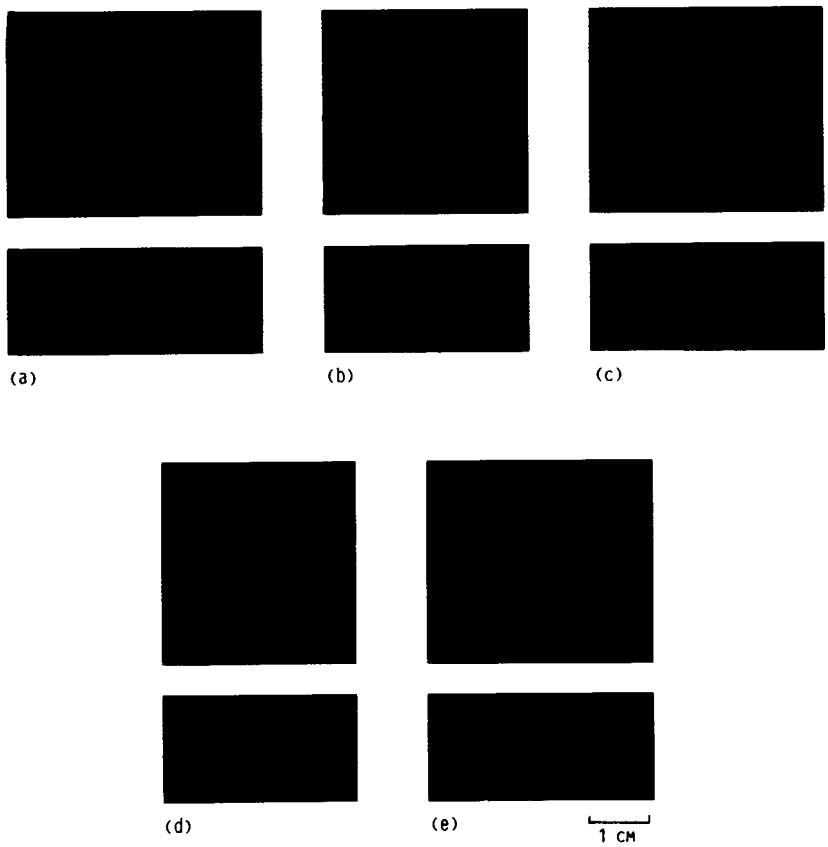

(a) Oxygen concentration = 18 mole % and V_{ch} = 7.39 cm/sec.
(b) Oxygen concentration = 18 mole % and V_{ch} = 4.32 cm/sec.
(c) Oxygen concentration = 17 mole % and V_{ch} = 6.72 cm/sec.
(d) Oxygen concentration = 17 mole % and V_{ch} = 3.57 cm/sec.
(e) Oxygen concentration = 16 mole % and V_{ch} = 6.15 cm/sec.

Figure 13.—Flames on 10-cm fuel samples in microgravity at various oxygen concentrations and characteristic relative velocities.

ORIGINAL PAGE
COLOR PHOTOGRAPH

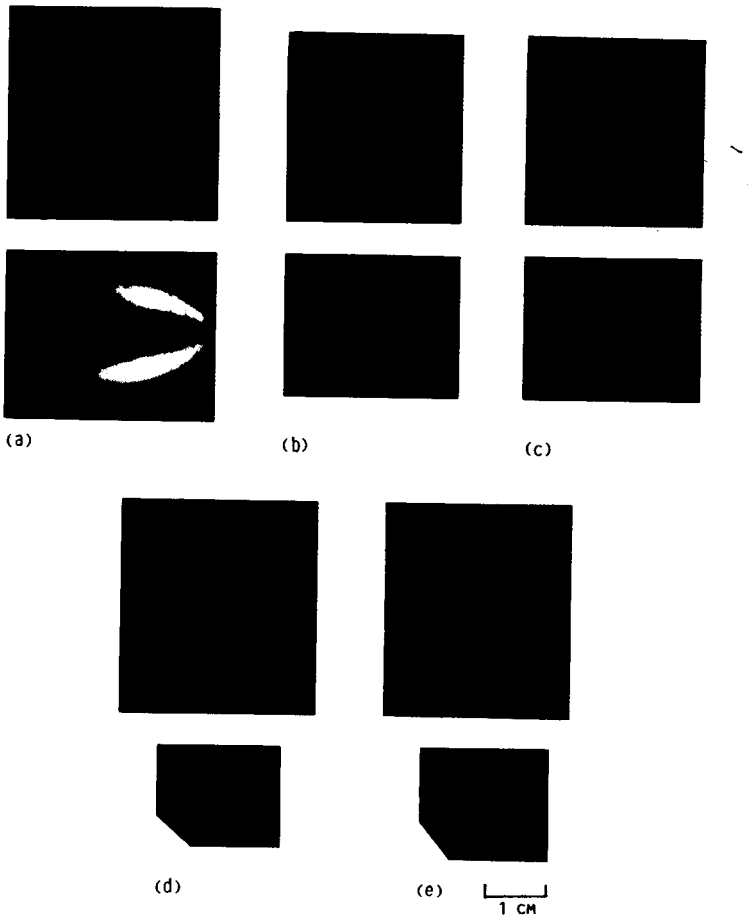

(a) Oxygen concentration = 21 mole % and V_{ch} = 6.93 cm/sec.
(b) Oxygen concentration = 18 mole % and V_{ch} = 2.05 cm/sec.
(c) Oxygen concentration = 17 mole % and V_{ch} = 1.52 cm/sec.
(d) Oxygen concentration = 15 mole % and V_{ch} = 5.66 cm/sec.
(e) Oxygen concentration = 15 mole % and V_{ch} = 4.28 cm/sec.

Figure 14.—Flames on 7-cm fuel samples in microgravity at various oxygen concentrations and characteristic relative velocities.

ORIGINAL PAGE
COLOR PHOTOGRAPH

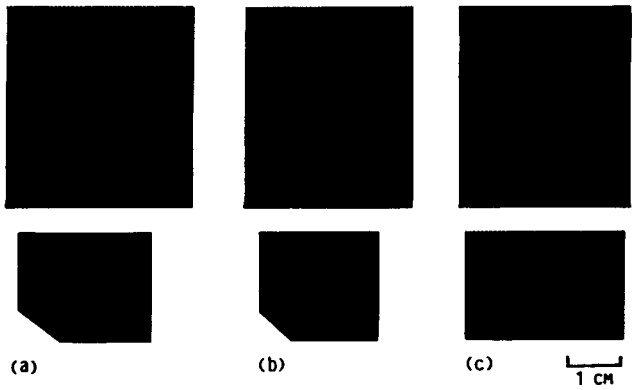

(a) Oxygen concentration = 14 mole % and V_{ch} = 6.08 cm/sec.
(b) Oxygen concentration = 14 mole % and V_{ch} = 4.19 cm/sec.
(c) Oxygen concentration = 17 mole % and V_{ch} = 0.81 cm/sec.

Figure 15.—Three microgravity flames prior to extinction.

smoldering appeared. The smoldering then weakened and disappeared, thereby indicating that combustion had indeed ceased.

Flame Spread In Air

Figure 16 presents three flames spreading in air at different characteristic relative velocities. Figure 16 parts (a) and (c), taken from reference 4, are photos of a microgravity quiescent flame and a normal-gravity downwardly propagating flame, respectively. Figure 16(b) is a microgravity flame in a slow-speed forced convection environment. The characteristic relative velocities for the three flames in figure 16 are 0.54, 6.93, and 89.1 cm/sec for (a) to (c), respectively. For the case of the flame spreading in normal gravity, the magnitude of the buoyant velocity induced in the flame zone was estimated and used as the characteristic relative velocity. The magnitude of the flow velocity had a very dramatic influence on the flame. Figure 16(a) shows a flame that exists at the lowest allowable oxygen mole fraction for microgravity quiescent flame spread, which is thus a limiting point. This limit is hereafter termed the quench limit. The flame was quite dim and was stabilized 2.5 mm from the fuel surface. Generating a mild free stream velocity (fig. 16) was enough to strengthen the flame and even seemed to induce some soot formation. This flame standoff distance was 1.2 mm from the fuel surface. The normal-gravity flame (fig. 16(c)) was very sooty, with a standoff distance less than the 0.36-mm fuel holder half-thickness.

Figure 17 presents flame spread rates on a thin fuel in air over a wide range of forced flow velocities. The plot includes the spread rates taken from the three flames shown in figure 16 as well as elevated-gravity data from Altenkirch (ref. 8). The spread rates of the elevated-gravity flames are corrected by using the flame spread formula derived by DeRis (ref. 9), which states that the flame spread rate should be inversely proportional to the area density of the fuel bed. The characteristic relative velocity shown covers the entire flammable range of the thin fuel in air, from the microgravity quiescent flame spread quench limit to the high-gravity blowoff limit. The shape of the curve indicates that the flame spread rate does not change monotonically with increasing characteristic relative velocity.

Figure 18 is a similar plot, but instead of elevated-gravity natural convection data, it includes normal-gravity, high-speed, horizontal, convective-flame-spread data from reference 7. The shape of the curve resembles the one in figure 17 if the points within the dotted lines at the top of the curve are removed. The rationale for doing this is that the low flow velocities indicated in this range may be an unrealistically low measure of the characteristic relative velocity; this is a reasonable assumption since natural convection, which is not considered, induces an additional flow that adds to the imposed flow.

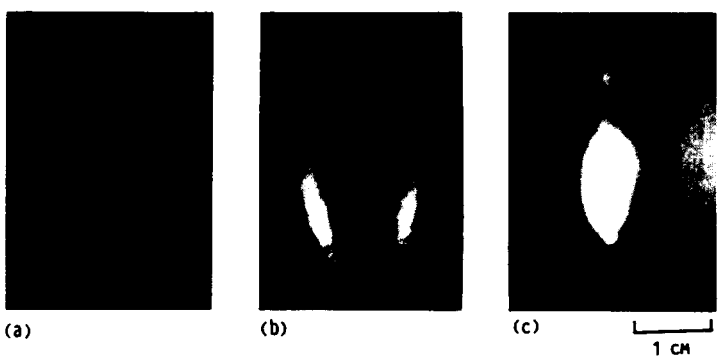

(a) Microgravity quiescent environment, V_{ch} = 0.54 cm/sec (ref. 4).
(b) Microgravity forced convection environment, V_{ch} = 6.93 cm/sec.
(c) Normal-gravity natural convection environment, V_{ch} = 89.1 cm/sec. (ref. 4).

Figure 16.—Direct photograph of three spreading flames in air.

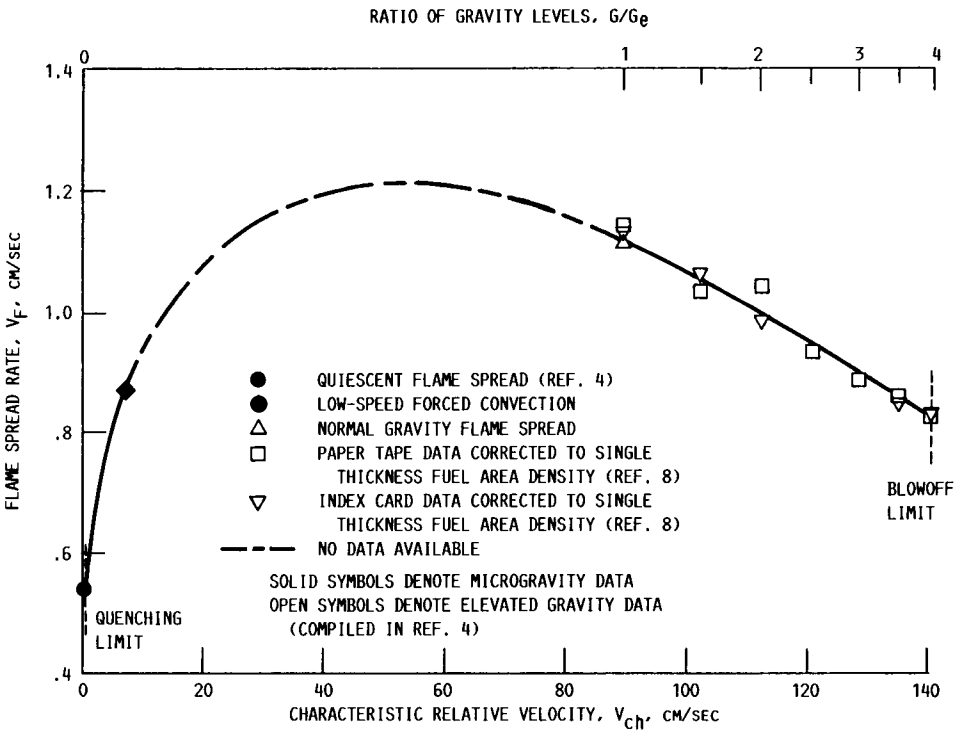

Figure 17.—Effect of flow on flame spread rate over a thin fuel in air.

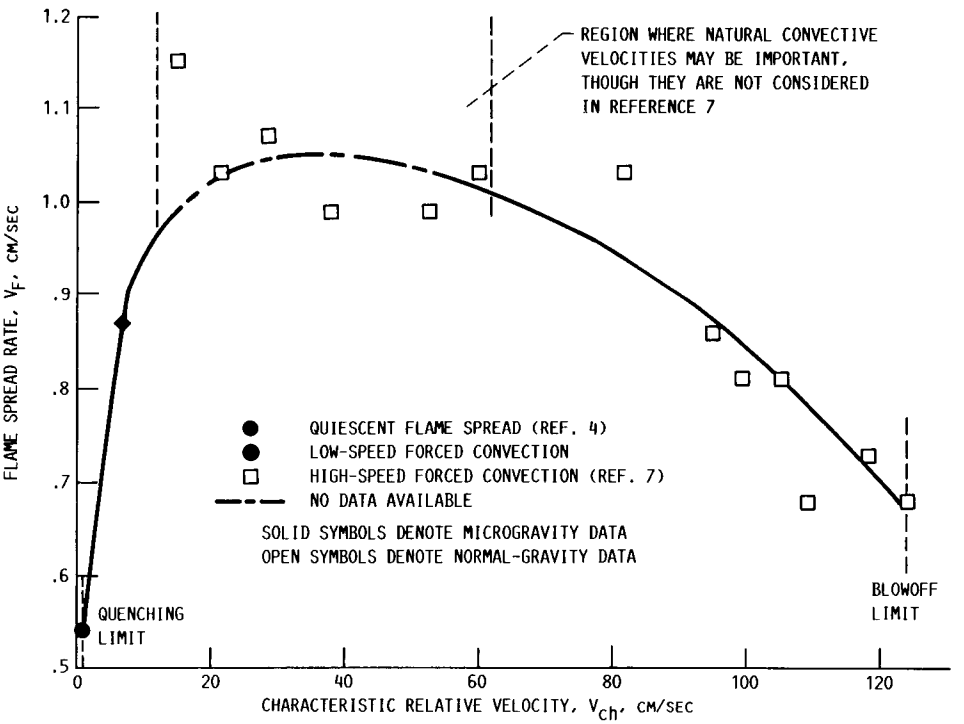

Figure 18.—Effect of flow on flame spread rate over a thin fuel in air.

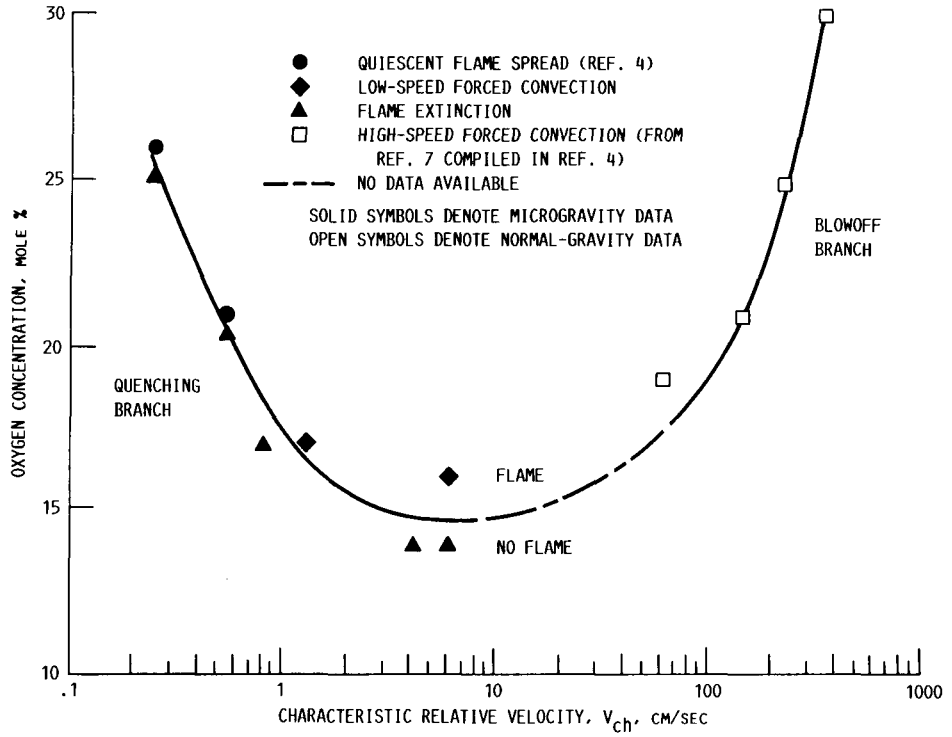

Figure 19.—Extinction boundary for flame spread over a thin cellulose fuel.

Flammability Map

Figure 19 represents the flammability boundary of a thin cellulose fuel with characteristic relative velocity and molar percentage oxygen as coordinates. It includes the microgravity quiescent flame-spread data from reference 4 and the high-speed forced convection data from reference 7. The blowoff and quenching extinction limits are indicated. A total of five quenching extinctions, three from this work and two from reference 4, define the quenching branch. The plot shows that there is a low molar percentage oxygen limit at around 15 percent. The shape of the curve resembles that predicted by T'ien (ref. 1).

Concluding Remarks

A diffusion flame established on a thin fuel in a low-speed forced flow in microgravity was studied. The data obtained were combined with that of previous experiments in microgravity, normal gravity, and elevated gravity to provide information on flame spread on a thin fuel over a wide range of flow conditions.

Existence of Quench Limit

For most opposed flow diffusion flames burning in the normal gravitational environment of Earth, the flow velocities induced by buoyancy are quite large. The Damkohler number (ratio of flow time to chemical reaction time) is sufficient to predict the flame spread and extinction characteristics of these flames (refs. 10 and 11). For a given oxidizer environment, blowoff occurs when the flow velocity becomes excessive, or equivalently, when the Damkohler number decreases sufficiently. The flame goes out because the gas residence time becomes too small. Thus, the chemical reactions are unable to keep pace with the rapid flow of oxidizer.

A low-speed quench limit (as previously reported by Olson (ref. 4)) was observed. This mode of extinction is quite different from that encountered in blowoff. In the quenching region the flow speed is quite low, so the gas residence time is large; thus, the Damkohler number is large. As determined by T'ien (ref. 1), extinction is caused by flame temperature reduction due to heat loss. This heat loss must be accounted for to predict both quenching extinction and flame spread characteristics in the quench limit region. Thus, in addition to the Damkohler number, a heat loss parameter should be considered.

Extinction Boundary

By placing the blowoff and quench extinction boundaries on one plot, a flammability map of a thin cellulosic fuel over a wide range of flow conditions and environments was obtained. The flammable region narrows with decreasing oxygen percentage until the blowoff and quench branches merge at some limiting value. Below this oxygen percentage, the fuel will not burn at any flow speed.

As indicated earlier, for two test conditions (marked with a *U* in fig. 6) the spread rates were undeterminable. This suggests that either the flames were in transition to extinction at the end of the microgravity test time, or that the flames were indeed stabilized at some very small spread rate. Because of this uncertainty, these two points were not used in constructing the extinction boundary.

It is significant that, for a given ambient oxygen concentration, a flame can be established in microgravity but not in normal gravity. The reason is that the buoyancy-induced velocities in normal gravity may lead to blowoff extinction, so by eliminating gravity and imposing a flow slower than that induced by buoyancy, a range of conditions is created that enables the flame to exist.

Recommendations

The effect of various parameters in the region near the quench limit need to be better quantified. Primarily, an accurate method of determining heat loss from the flame is important. This will aid in predicting flame spread and extinction characteristics. Also needed are flame temperature measurements and a determination of the effect of velocity profile on the flame spread process.

Acknowledgments

This work would not have been possible without the help of a NASA Graduate Student Researchers Grant (NGT-50088), for which I am very grateful. I would like to thank Raymond Sotos of NASA Lewis Research Center for helping in the design of the apparatus and fabricating it.

Appendix—Experimental Error

The measured quantities were position, time, and pressure. From these, all relevant data were extracted.

The measurement of the position of a given point has already been outlined in the discussion of the apparatus. The accuracy of the measurement depends on the sharpness of the image. For example, the boundary of a dim, diffuse flame is more difficult to determine than the edge of a well-lit solid object.

To determine position error, repeated measurements of a very dim point on the flame were made. The error was taken to be half of the spread between the largest and smallest value recorded. This error was ± 0.05 cm. Since all length measurements are merely the difference between two position readings, the overall uncertainty is ± 0.1 cm.

Time was measured with the framing rate of the camera, which was always set at 24 frames/sec. To verify the framing rate, the total number of frames for the 5.18-sec drop time were counted. There were 124 frames for the given framing rate. Time was used to compute the speed of the flame relative to the fuel (flame spread rate) and the speed of the fuel into the quiescent environment.

To estimate the error in the velocity measurements, a least squares linear fit of the position as a function of time data was obtained. The slope of the line yielded the magnitude of the velocity, and the error was taken to be twice the standard deviation of the curve fit. The errors encountered ranged from 0.06 to 0.2 cm/sec for the fuel velocity and from 0.08 to 0.15 cm/sec for the flame spread rates.

A linear fit of the position as a function of time data was justified for the fuel speed since the drive motor was designed to produce a constant speed. The flame spread rate, however, was not necessarily constant, especially for flames near the extinction limit. The flame spread rates tended to vary slightly about some mean value. This was also observed by Olson (ref. 4). Thus the reported spread rate is actually the average value.

The oxygen mole fraction was determined by using the fact that the partial pressure of a perfect gaseous component equals the product of its mole fraction and the total pressure. The evacuated combustion vessel was first filled to the required partial pressure of oxygen and then filled to 1 atm pressure with nitrogen. The uncertainty in the mole fraction depends on the accuracy of the pressure gage, which is ± 0.01 psi. This translates into an uncertainty of ± 0.1 percent for the range of molar oxygen percentages required in this experiment.

References

1. T'ien, J.S.: Diffusion Flame Extinction at Small Stretch Rates: The Mechanism of Radiative Loss. Combust. Flame, vol. 65, no. 1, July 1986, pp. 31-34.
2. Bonne, U.: Radiative Extinguishment of Diffusion Flames at Zero Gravity. Combust. Flame, vol. 16, no. 2, Apr. 1971, pp. 147-159.
3. Foutch, D.: Size and Shape of Solid Fuel Diffusion Flames in Very Low Speed Flows. Master of Science Thesis, Case Western Reserve University, NASA CR-179576, 1986.
4. Olson S.L.: The Effect of Microgravity on Flame Spread over a Thin Fuel. Master of Science Thesis, Case Western Reserve University, NASA TM-100195, 1987.
5. Chen, C.H.: Diffusion Flame Extinction in Slow Convective Flow under Microgravity Environment. NASA TM-88799, 1986.
6. Rosenhead, L., ed.: Laminar Boundary Layers. Oxford University Press, 1963, pp. 360-362.
7. Fernandez-Pello, A.C.; Ray, S.R.; and Glassman, I.: Flame Spread in an Opposed Forced Flow: The Effect of Ambient Oxygen Concentration. 18th Symposium (International) on Combustion, The Combustion Institute, 1981, pp. 579-589.
8. Altenkirch, R.A.; Eichorn R.; and Shang, P.C.: Buoyancy Effects on Flames Spreading Down Thermally Thin Fuels. Combust. Flame, vol. 37, no. 1, Jan. 1980, pp. 77-83.
9. DeRis, J.N.: Spread of a Laminar Diffusion Flame. 12th Symposium (International) on Combustion, The Combustion Institute, 1969, pp.241-252.
10. Fernandez-Pello, A.C.; and Hirano, T.: Controlling Mechanisms of Flame Spread. Combust. Sci. Technol., vol. 32, nos. 1-4, 1983, pp. 1-31.
11. Fernandez-Pello, A.C.: Flame Spread Modeling. Combust. Sci. Technol., vol. 39, 1984, pp. 119-134.

NASA
National Aeronautics and Space Administration

Report Documentation Page

1. Report No.	2. Government Accession No.	3. Recipient's Catalog No.
NASA CR-182185		

4. Title and Subtitle
An Experimental Study of Opposed Flow Diffusion Flame Extinction Over a Thin Fuel in Microgravity

5. Report Date
February 1989

6. Performing Organization Code

7. Author(s)
Paul V. Ferkul

8. Performing Organization Report No.
None (E-4440)

10. Work Unit No.
674-22-05

9. Performing Organization Name and Address
Case Western Reserve University
Department of Mechanical and Aerospace Engineering
Cleveland, Ohio 44106

11. Contract or Grant No.
NGT-50088

13. Type of Report and Period Covered
Contractor Report
Final

12. Sponsoring Agency Name and Address
National Aeronautics and Space Administration
Lewis Research Center
Cleveland, Ohio 44135-3191

14. Sponsoring Agency Code

15. Supplementary Notes
Project Manager, Sandra L. Olson, Space Experiments Division, NASA Lewis Research Center. Paul V. Ferkul, NASA Resident Research Associate. This report was a thesis submitted in partial fulfillment of the requirements for the degree of Master of Science to the Department of Mechanical and Aerospace Engineering, Case Western Reserve University, in August 1988.

16. Abstract
An experiment was conducted to examine the flame spread and flame extinction characteristics of a thin fuel burning in a low-speed forced convective environment in microgravity. The flame spread rate was observed to decrease both with decreasing ambient oxygen concentration as well as decreasing free stream velocity. A new mode of flame extinction was observed, caused by either of two means: keeping the free stream velocity constant and decreasing the oxygen concentration, or keeping the oxygen concentration constant and decreasing the free stream velocity. This extinction is called quenching extinction. By combining this data together with a previous microgravity quiescent flame study and normal-gravity blowoff extinction data, a flammability map was constructed with molar percentage oxygen and characteristic relative velocity as coordinates. The Damkohler number is not sufficient to predict flame spread and extinction in the near quench limit region.

17. Key Words (Suggested by Author(s))	18. Distribution Statement
Combustion Microgravity Flame spread Extinction	Unclassified – Unlimited Subject Category 25

19. Security Classif. (of this report)	20. Security Classif. (of this page)	21. No of pages	22. Price*
Unclassified	Unclassified	16	A03

NASA FORM 1626 OCT 86

*For sale by the National Technical Information Service, Springfield, Virginia 22161